Int J Earth Sci (Geol Rundsch) (2017) 106:2461–2471
DOI 10.1007/s00531-016-1442-9

ORIGINAL PAPER

Superposition of tectonic structures leading elongated intramontane basin: the Alhabia basin (Internal Zones, Betic Cordillera)

Manuel Martínez-Martos[1,2] · Jesús Galindo-Zaldivar[1,2] · Francisco José Martínez-Moreno[3] · Raquel Calvo-Rayo[1] · Carlos Sanz de Galdeano[2]

Received: 20 September 2016 / Accepted: 22 December 2016 / Published online: 20 January 2017

Abstract The relief of the Betic Cordillera was formed since the late Serravallian inducing the development of intramontane basins. The Alhabia basin, situated in the central part of the Internal Zones, is located at the intersection of the Alpujarran Corridor, the Tabernas basin, both trending E–W, and the NW–SE oriented Gádor–Almería basin. The geometry of the basin has been constrained by new gravity data. The basin is limited to the North by the Sierra de Filabres and Sierra Nevada antiforms that started to develop in Serravallian times under N–S shortening and to the south by Sierra Alhamilla and Sierra de Gádor antiforms. Plate convergence in the region rotated counter-clockwise in Tortonian times favouring the formation of E–W dextral faults. In this setting, NE–SW extension, orthogonal to the shortening direction, was accommodated by normal faults on the SW edge of Sierra Alhamilla. The Alhabia basin shows a cross-shaped depocentre in the zone of synform and fault intersection. This field example serves to constrain recent counter-clockwise stress rotation during the latest stages of Neogene–Quaternary basin evolution in the Betic Cordillera Internal Zones and underlines the importance of studying the basins' deep structure and its relation with the tectonic structures interactions.

✉ Manuel Martínez-Martos
manuelmm@ugr.es

[1] Departamento de Geodinámica, Universidad de Granada, 18071 Granada, Spain

[2] Instituto Andaluz de Ciencias de la Tierra, CSIC-Universidad de Granada, Avenida de las Palmeras, no 4, 18100 Armilla, Spain

[3] Faculdade de Ciências, IDL-Universidade de Lisboa, Campo Grande, Ed. C8, Lisbon, Portugal

Keywords Basin geometry · Gravity prospecting · Superimposed sedimentary basins · Recent tectonic evolution

Introduction

Orogenic intramontane basins record regional tectonic evolution and deformation patterns over time. They are filled by sediments either in synformal structures perpendicular to compression (Burg and Podladchikov 1999; Guest et al. 2007), in grabens orthogonal to extension (Carmignani et al. 2004) or in pull-apart basins related to wrench regimes (Jacobs and Thomas 2004). Due to the interaction and overlapping of such tectonic features, intramontane basins may cross-cut one another, leading to superimposed basins. Such basin interaction has been described in collisional orogens such as the Anatolian Fault Zone (Gurer et al. 2001; Yilmaz and Gelisli 2003; Tari et al. 2013) or the Balkan Peninsula (Zagorčev 1992). Superimposed basins in collisional contexts are usually a consequence of an advanced orogenic stage and/or a complex deformational history.

In the Betic Cordillera of southern Spain (Fig. 1), intramontane basins developed due to relief uplift since the late Tortonian (Braga et al. 2003; Sanz de Galdeano and Alfaro 2004; Pedrera et al. 2007). Elongated basins are often close to the highest reliefs of the Internal Zones. The interaction between faults and folds in the Betic Cordillera gave rise to the formation of superimposed intramontane basins (Galindo-Zaldivar et al. 2003). In the Central–Eastern Betic Cordillera, three intramontane elongated basins intersect: the Alpujarran Corridor, the Tabernas basin and the Gádor–Almería basin. In this study, we denominate the

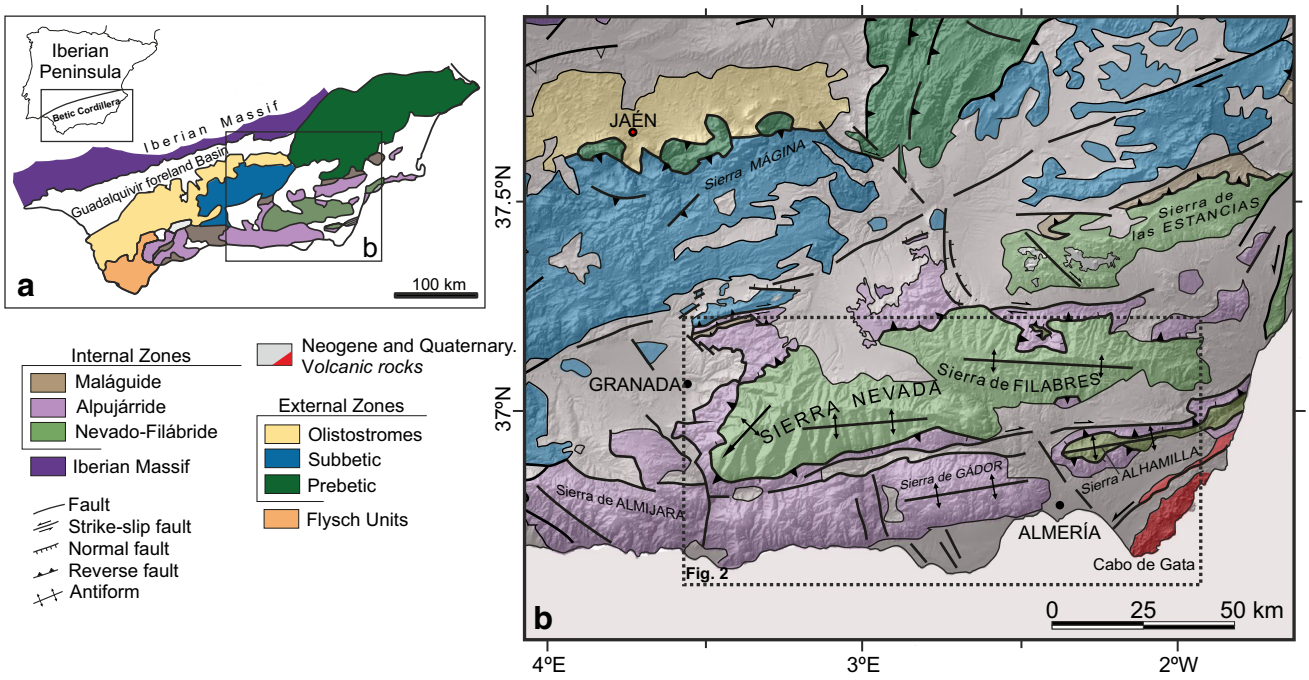

Fig. 1 Geological setting of the central and eastern Betic Cordillera. **a** Geological sketch of the Betic Cordillera. **b** Geological map with main geological structures

intersection of these intramontane basins as the Alhabia basin (Fig. 2).

The Alpujarran Corridor is a mainly dextral-faulted synformal structure that separates the Sierra Nevada and the Sierra de Gádor antiforms (Sanz de Galdeano et al. 1985; Galindo-Zaldivar 1986; Sanz de Galdeano 1996; Rodríguez-Fernández et al. 1990; Martínez-Díaz 2000; García et al. 2003; Martínez-Díaz and Hernández-Enrile 2004; Martínez-Martínez 2006; Martínez-Martínez et al. 2006). The Tabernas basin is likewise a synformal structure, in this case separating the Sierra de Filabres and Sierra Alhamilla antiforms, yet it is south-bounded by a southward-dipping dextral reverse fault zone (Sanz de Galdeano 1989; Giaconia et al. 2012). This basin has also been widely studied to better understand the cordillera evolution and the exhumation of metamorphic bedrock in the area (Weijermars et al. 2007; Do Couto et al. 2014). The Gádor–Almería basin, in turn, separates the Sierra de Gádor and Sierra Alhamilla antiforms and is formed by NW–SE normal faults (Marín-Lechado et al. 2005; Pedrera et al. 2006). GPS research provides evidence that the region is affected by a westward displacement with regard to the stable Iberian Massif (Fig. 2) (Echeverria et al. 2013; Galindo-Zaldivar et al. 2015).

Although these basins have been previously studied from tectonic and stratigraphic points of view, applications of geophysical prospection to determine their structure are scarce. Gravity research has been undertaken in the central Alpujarran Corridor (Ruiz Constán et al. 2013), in the eastern Tabernas basin (Li et al. 2012; Do Couto et al. 2014) and in the Gádor–Almería basin (Pedrera et al. 2006), but to date it does not cover the intersection of these three elongated basins.

The aim of this paper was to establish the geometry of the Alhabia basin and discuss its tectonic evolution. To constrain the variation in thickness of the sedimentary infill, we carried out gravity measurements along several profiles and performed 2D forward models. These new geophysical data enable us to evaluate the influence of recent and active faults and folds on the latest tectonic evolution of the Betic Cordillera. This field example illustrates the importance of elongated intramontane basins to elucidate the cordilleras regional evolution.

Geological setting

The Betic Cordillera is located in the westernmost part of the Mediterranean Alpine Orogen (Fig. 1). Its origin lies in the Africa–Eurasia plate convergence, thereby constituting an example of continental collision (Ruiz-Constán et al. 2012). Two main controversial models have been proposed to explain this orogen formation: models based on subduction with associated roll-back detachment of the subducting slab (Ruiz-Constán et al. 2011; Gonzalez-Castillo et al. 2015) and models based on lithospheric delamination of

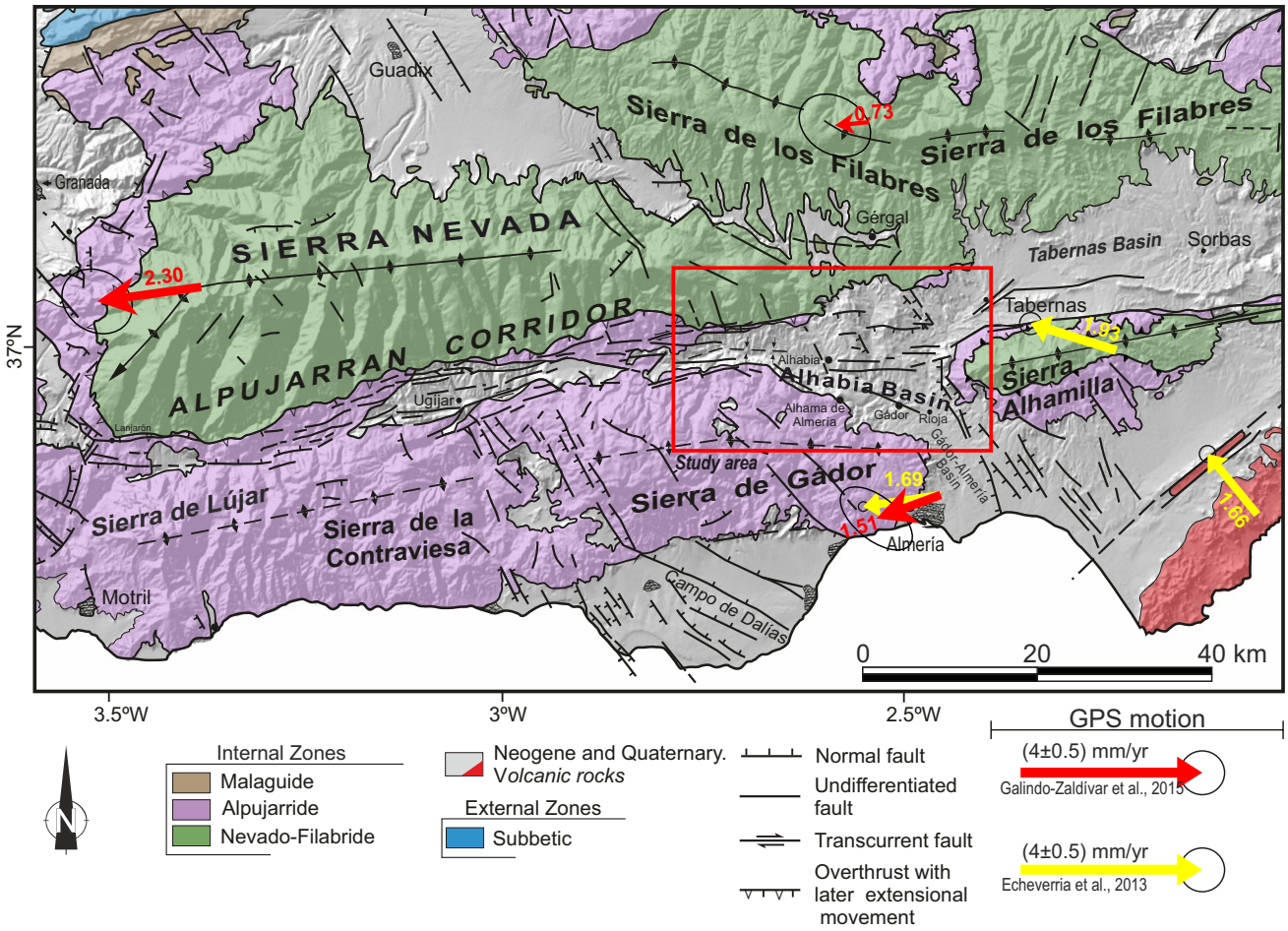

Fig. 2 Geological map of the Alhabia Basin including CGPS (*red*) and GPS (*yellow*) arrows with their 95% confidence ellipses, respectively, from Galindo-Zaldivar et al. (2015) and Echeverria et al. (2013)

subcontinental lithosphere beneath the Alboran Sea (Calvert et al. 2000; Mancilla et al. 2013). The Betic Cordillera is divided into the Internal and External Zones and the Flysch Units. The Internal Zone comprises three main metamorphic complexes of Palaeozoic and Mesozoic rocks—from bottom to top, the Nevado-Filábride, Alpujárride and Maláguide complexes—in addition to the Pre-dorsal and Dorsal complexes (Azañón et al. 2002).

During lower Serravallian, in a first stage of relief development along the South Iberian Margin, the Mediterranean Sea and the Atlantic Ocean were connected by the North-Betic Strait—located at the former Guadalquivir basin (Sanz de Galdeano and Vera 1991, 1992)—and the North-Betic basin (Soria 1998). From the late Miocene to the Quaternary, most of the intramontane basins became isolated by the continuous deformation related to Africa–Eurasia convergence (Vera 2000).

The large relief of Sierra Nevada, Sierra de Filabres, Sierra de Gádor and Sierra Alhamilla were uplifted by E–W to NE–SW antiforms during the Miocene, and E–W dextral faults developed (Sanz de Galdeano 1996), creating synformal depressed areas such as the Alpujarran Corridor and the Tabernas basin (Weijermars et al. 2007; Sanz de Galdeano and Alfaro 2004; Pedrera et al. 2012). In addition, E—W normal faults with a dextral component affected Neogene–Quaternary sediments along the eastern Alpujarran Corridor (Sanz de Galdeano et al. 2010). Moreover, E–W reverse-dextral faults deform the southern border of the Tabernas basin (Sanz de Galdeano 1989; Giaconia et al. 2012). NW–SE normal faults in the study area are located between Sierra de Gádor and Sierra Alhamilla, contributing to the formation of the Gádor–Almería basin and merging it with the Alpujarran Corridor and the Tabernas basin (Pedrera et al. 2006; Marín-Lechado et al. 2005).

Unconformable sediments fill the intramontane basins developed in between these sierras (Fig. 2). In the Alhabia basin, the lowest sediments correspond to Burdigalian to Serravallian patches (Kleverlaan 1987, 1989). Atop these sediments, late Tortonian calcareous sandstones and marly calcarenites were unconformably deposited (Ruegg 1964),

followed by Messinian reefs in the southwesternmost part. The upper Messinian deposits include evaporites, covered by Pliocene continental conglomerates, sands and silts (Martin and Braga 1994). During the latest Pliocene and the early Pleistocene, the study area has emerged and deposits developed only in rivers and ravines.

Methods

Gravity prospecting was carried out to estimate the Alhabia basin geometry. The measurement site positions were determined by means of differential GPS. In addition, direct field observations (Fig. 3) helped to link the outcropping tectonic structures to the deep basin geometry.

Gravity prospecting makes it possible to determine the geometry of bodies with contrast of density. Sedimentary infill of the Alhabia basin has lower density than the metamorphic basement. A total of 475 new gravity measurements were obtained, mainly along N–S and NE–SW profiles, roughly orthogonal to the main tectonic features and basin boundaries and along the most accessible paths. Some additional stations between the profiles were considered to improve the gravity anomaly maps (Fig. 4). The gravimeter used was a Scintex Autograv CG-5, which has 1 μGal of accuracy. The obtained measurements were referred to the absolute gravity station of Granada (National Geographical Service of Spain, IGN, http://www.ign.es). Free Air, Bouguer and Terrain corrections were calculated for each gravity site using a standard terrain density of 2.67 g/cm^3 (Martínez-Moreno et al. 2016). The Terrain correction was derived combining the methods developed by Kane (1962) and Nagy (1966) up to 160 km around each gravity site, using the 5-m accuracy DEM provided by the IGN (http://www.ign.es). After applying corrections, the Bouguer anomaly map of the study area was obtained (Fig. 4a). The regional anomaly map (Fig. 4b) was obtained by kriging the gravity data located in the bedrock

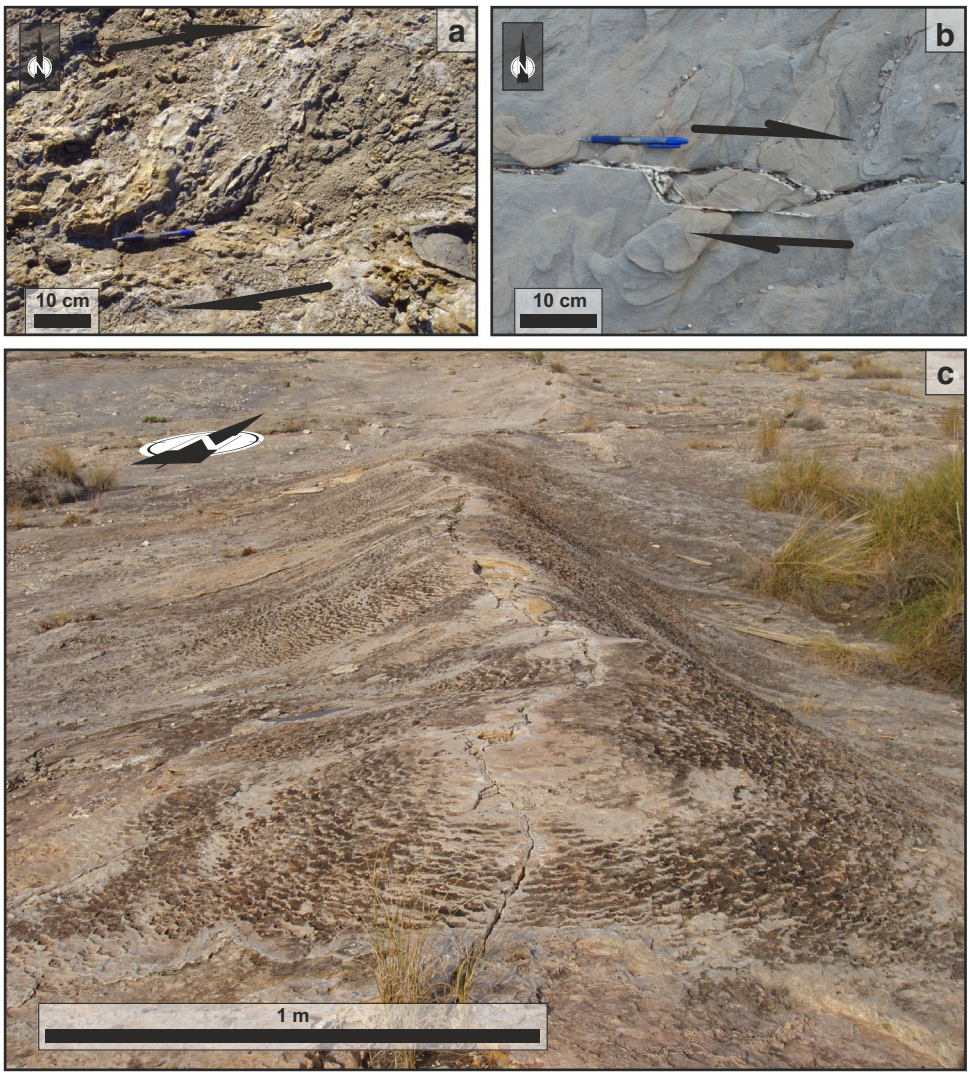

Fig. 3 Field examples of tectonic structures. **a** S-C and **b** dextral off-set seen in plain view on Miocene sediments. **c** Example of present-day travertines related to a NW–SE trending fracture in the northeast part of the Alhabia Basin

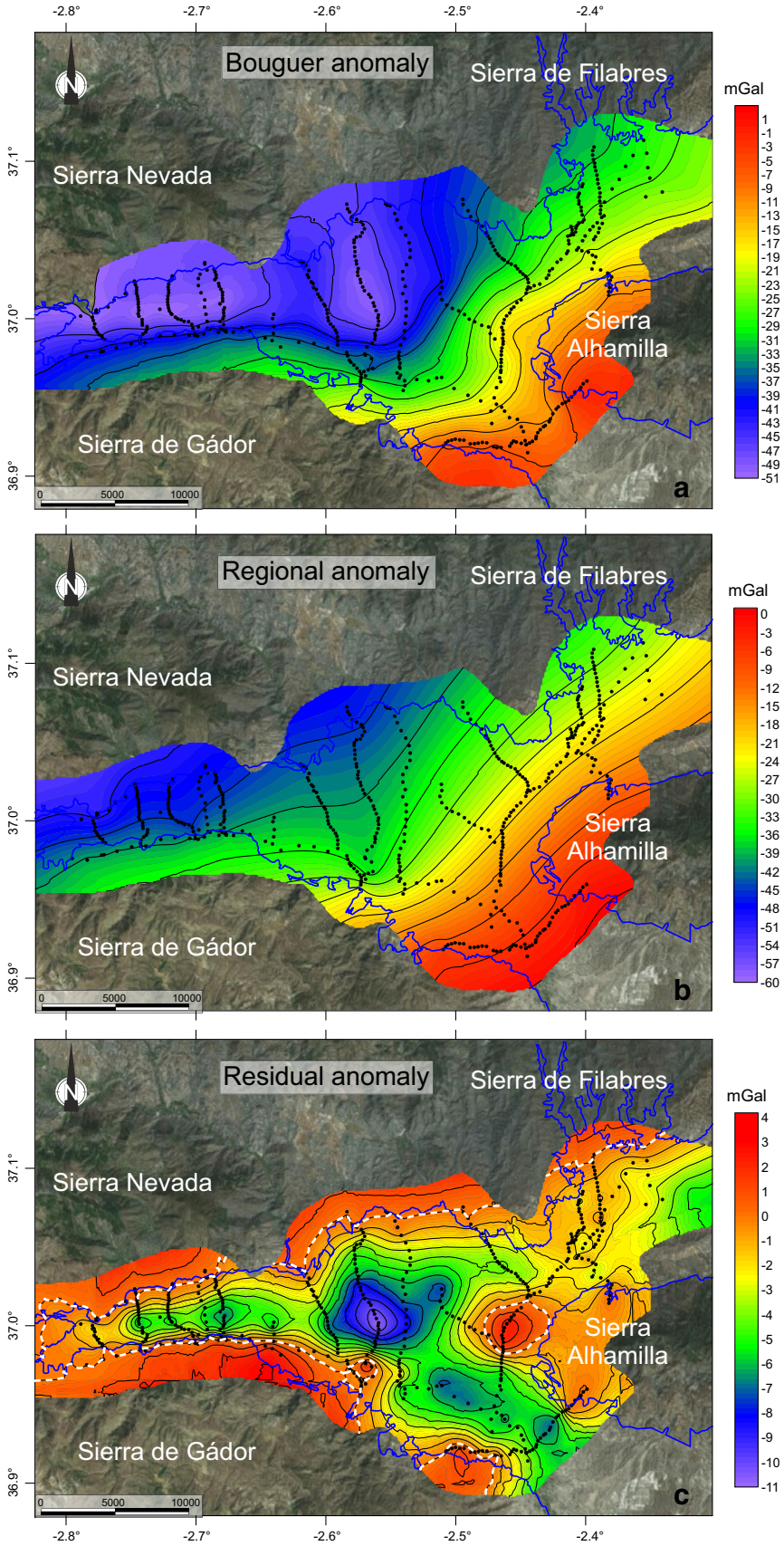

Fig. 4 Gravity anomaly maps. *Black dots* show the location of gravity measurements and *blue line* indicates the basin's boundaries. **a** Bouguer anomaly map and its separation into **b** regional anomaly map and **c** residual anomaly map. *White-dashed line* shows the residual anomaly 0 value

(Martínez-Moreno et al. 2015). The residual anomaly map was derived from the difference between the Bouguer and the regional anomaly maps (Fig. 4c).

2D forward models were obtained using GravMag v.1.7 software (Pedley et al. 1993). The densities used to model were 2.25 g/cm^3 for the sedimentary infill and 2.67 g/cm^3 for the bedrock, in view of previous studies in the area (Marín-Lechado et al. 2007; Pedrera et al. 2009; Li et al. 2012; Ruiz-Constán et al. 2013; Do Couto et al. 2014) and according to standard values (Telford et al. 1990). In addition, we present alternative gravity models to assess the uncertainty in the sedimentary infill thickness determination, considering the maximum and minimum possible density values (from 2.00 to 2.40 g/cm^3). In any case, an average 2.25 g/cm^3 density for the sedimentary infill has been estimated to provide the most suitable results. The standard deviation (SD) and RMS error have been calculated for each gravity model with the proposed sedimentary infill density at 2.25 g/cm^3 (Fig. 5).

Structure of the Alhabia basin

Field observations on main faults

E–W and NW–SE faults are superposed in the Alhabia basin, although they have different ages (Sanz de Galdeano et al. 2010). E–W faults are common in the northern part of the study area, affecting the Alpujarran Corridor and Tabernas basin sediments. These faults present mainly dextral and locally normal slip, evidenced by striae together with S-C fabric and stretch marks affecting the Miocene and Pliocene sediments (Fig. 3a, b). Quaternary sediments are clearly affected by recent faults in the Alpujarran Corridor's central part (García-Tortosa and Sanz de Galdeano 2007). The NW–SE normal faults, however, present mainly dip slip. They are located in western part of the Tabernas basin and in the Gádor–Almería basin, deforming the sediments between Sierra de Gádor and Sierra Alhamilla (Marín-Lechado et al. 2005). These faults activity probably started during Tortonian time, affecting up to Quaternary sediments and allowing the development of travertines up to present times (Fig. 3c).

Basin infill geometry from gravity research

The values of the Alhabia basin Bouguer anomaly map (Fig. 4a) are between −51 and −2 mGal in agreement with regional Bouguer maps (e.g. IGN 1976; Ayala et al. 2016). Still, this map does not provide much information about the sedimentary infill because of the masking effect of the intense regional anomaly (Fig. 4b) related to southeastward crustal thinning from the Betic Cordillera towards the Alboran Sea (Torné and Banda 1992). The residual anomaly (Fig. 4c) values are between −10.6 and 2.3 mGal, and the 0 mGal line roughly coincides with the basin limits. It presents a cross-shaped minimum within the Alhabia basin, where the elongated basins merge together. Each branch of this cross-shaped minimum points to relative elongated minima, related to the Tabernas basin (eastward), the Gádor–Almería basin (southward), and the Alpujarran Corridor (westward). The northern branch, however, points to Sierra de Filabres and is poorly developed. The anomaly westward Tabernas basin and between Sierra Nevada and Sierra de Filabres is very minor, supporting a thinner sedimentary cover.

Three residual gravity anomaly profiles were modelled to highlight the structure of the gravity minima related to the western and southern depocentre branches (Fig. 5). The N–S profiles (P1 and P2 in Fig. 5a) transect the Alpujarran Corridor´s westernmost part, from Sierra Nevada to Sierra de Gádor, whereas the NE–SW profile (P3 in Fig. 5a) cross-cuts the Gádor–Almería basin from Sierra de Gádor to Sierra Alhamilla. Profile 1 is asymmetric, with a gradual residual anomaly decreasing southward from Sierra Nevada, reaching a minimum value of −7 mGal, yet showing an abrupt increase towards the Sierra de Gádor. Profile 2 is located the eastern Alhabia basin and presents a pronounced minimum of −10.6 mGal displaced southwards. A noteworthy characteristic of this profile is the presence of a local maximum of 2 mGal in the southern part of the sedimentary infill. Profile 3 is also asymmetric, presenting its minimum value displaced towards the NE. There is a gradual decrease in value of −7.5 mGal from Sierra de Gádor eastwards, with an abrupt increase at the Sierra Alhamilla boundary.

Gravity models for profiles 1, 2 and 3 (Fig. 5) reveal the sedimentary infill geometry (2.25 g/cm^3) on top of the metamorphic basement (2.67 g/cm^3). The positive residual anomaly maximum at ~11 km length in profile 2 suggests the presence of a high-density body (2.9 g/cm^3) in the southern part of the metamorphic basement.

Discussion

The Alhabia basin illustrates the interaction and evolution of tectonic structures in complex collisional orogens, with the development of cross-cutting elongated basins. Intramontane basins are the shallow expression of crustal deformation in collisional contexts. The Betic Cordillera Internal Zones was deformed by several tectonic structures favouring the development of elongated basins. In the Alhabia basin, the E–W Alpujarran Corridor—in continuity to Tabernas basin—is connected to the NW–SE Gádor–Almería basin (Fig. 2). The Alpujarran Corridor

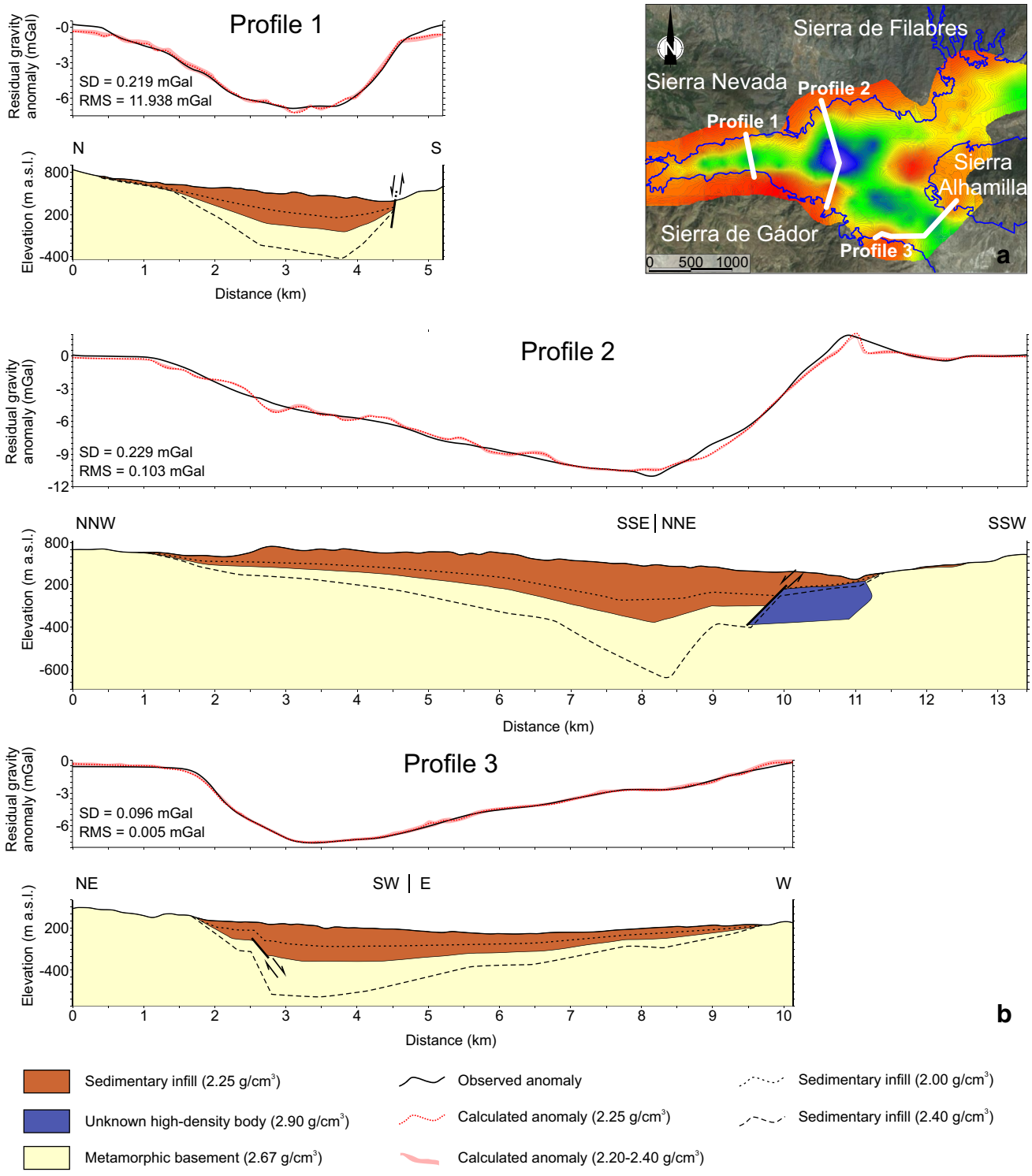

Fig. 5 Gravity survey modelling in the study area. **a** Location of residual anomaly profiles and **b** their observed/calculated residual anomaly fitting (*top*) with their related models (*bottom*)

formed as a faulted synformal structure between Sierra Nevada and Sierra de Gádor antiforms due to the N–S to NW–-SE Africa–Eurasia convergence (Sanz de Galdeano et al. 1985; Galindo-Zaldivar 1986; Sanz de Galdeano 1996; Martínez-Díaz and Hernández-Enrile 2004; Martínez-Martínez 2006). Faults developed afterwards, with normal and dextral components, due to extension orthogonal to the NW–SE compression that was probably

related to the relief uplift (García-Tortosa and Sanz de Galdeano 2007).

The Tabernas basin appears to have a similar initial evolution, in connection with the Alpujarran Corridor (Do Couto et al. 2014; Li et al. 2012). However, it features the remarkable presence of a dextral-reverse fault zone at its southern boundary and the absence of active N–S extension recorded in the Alpujarran Corridor. The Gádor–Almería basin, situated between Sierra de Gádor and Sierra Alhamilla, is bounded by highly active NW–SE normal faults with related seismicity; they propagate northwestward and cross-cut the former E–W Alpujarran Corridor and the Tabernas basin (Sanz de Galdeano et al. 2010). Main fractures facilitate deep circulation and the presence of travertine deposits in the Alhabia basin (Sanz de Galdeano et al. 2008) (Fig. 3c).

The new gravity data reveal the deep Alhabia basin infill geometry. It is noteworthy the cross-shape structure of the depocentre that extends towards the Alpujarran Corridor and the Gádor–Almería basin. Two branches have scarce sedimentary infill: the eastern Tabernas basin and the northern branch towards Sierra de Los Filabres. Three geological models based on gravity data highlight these basins main characteristics. The model in profile 1 (Fig. 5) reveals the sedimentary infill accumulated in a synformal structure with a southward-displaced hinge zone, reaching a maximum sedimentary thickness of 450 m. In addition, an E–W normal highly dipping fault is located at the southern boundary of the basin. The model for profile 2 also reveals the thickest sedimentary infill of a synformal structure, reaching 800 m. The high-density body (2.9 g/cm^3) in the metamorphic bedrock related to the positive residual anomaly maximum at 11 km length may be related to mineralisations. This model also supports the presence of faults cross-cutting the southern part of the basin and causing the bedrock to crop out abruptly. Model 3 shows sedimentary infill gradually increasing in thickness towards the NE until reaching 500 m at 7 km from the beginning. Then, around Sierra Alhamilla a high-angle normal fault separates the sedimentary infill from the metamorphic basement (Fig. 2).

The gravity models reveal the asymmetry of the synform in the Alpujarran Corridor, with a depocentre located close to the south boundary. This asymmetry is consistent with the northward vergence observed in Sierra Nevada and Sierra Alhamilla folds (Jabaloy et al. 1993; Marín-Lechado et al. 2007; Pedrera et al. 2009). The presence of high-angle faults is also remarkable both in the southern part of the Alpujarran Corridor, with E–W orientations, and in the Gádor–Almería basin, NW–SE oriented. Together with the asymmetric synformal structures, these faults interacted and contributed to superimposed basin formation and to the uplift of the surrounding reliefs.

Active surface deformation is revealed by continuous GPS (Galindo-Zaldivar et al. 2015) and non-permanent GPS networks (Echeverria et al. 2013) (Fig. 2). They suggest differential displacements of the metamorphic blocks that surround the intramontane basins. Sierra de Filabres remains steady with respect to the Iberian Massif. Western Sierra Nevada moves westwards, with no major recent structures separating it from Sierra de Filabres. This motion has been interpreted as a widespread E–W stretching of the metamorphic basement due to the presence of N–S to NW–SE extensional joints (Galindo-Zaldivar et al. 2015), although it may also be favoured by the activity of the northwestward-propagating faults of the Gádor–Almería basin. Sierra de Gádor moves west-southwestward, according to the Alpujarran Corridor faults dextral and extensional character, evidencing the end of the synform development. Sierra Alhamilla moves towards the northwest, accommodating this displacement with reverse and dextral faults at its northern boundary, perhaps in conjunction with the latest stages of folding. Normal faults at the western edge determine the opening of the Gádor–Almería basin (Fig. 6).

Although basin superposition is a common phenomenon in collision orogens, most studied examples correspond to superimposed grabens as in the Balkan Peninsula (Zagorčev 1992) or the Anatolian Fault Zone (Gurer et al. 2001; Yilmaz and Gelisli 2003; Tari et al. 2013). However, in the Betic collision orogen, the elongated basin development is a consequence of the interaction between synform and faults. Metamorphic rocks crop out along antiforms that are separated by faulted synformal structures which, due to the relatively thinner crust, represent the weakest and most easily deformable areas to be faulted.

Conclusions

The Alhabia basin is a remarkable example of interacting elongated intramontane basins in a collisional orogen formed along main crustal weakness zones. According to new gravity data, field tectonic observations, and GPS motions, the recent deformations related to the E–W Alpujarran Corridor and the Tabernas basin intersection, together with the NW–SE oriented Gádor–Almería basin, produced a cross-shaped depocentre. In the context of Africa–Eurasia convergence, N–S compression formed large asymmetric folds verging northwards during late Serravallian-early Tortonian (Martín-Algarra et al. 2009). Counter-clockwise rotation of stresses to NW–SE compression, also including orthogonal extension, determines the propagation of new folds (Sierra de Gádor and Sierra

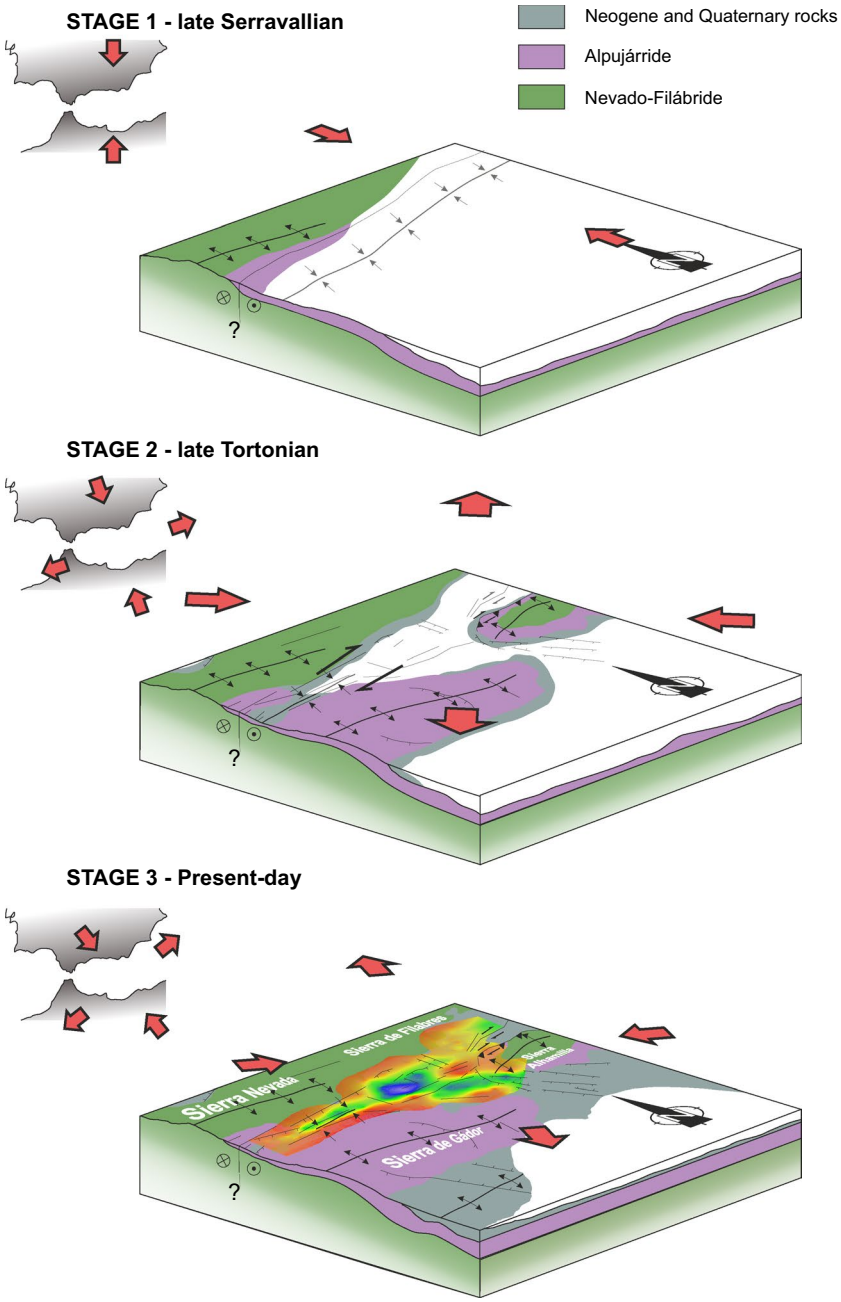

Fig. 6 Tectonic evolution in the Alhabia basin related to the Africa–Eurasia convergence changes over time. **a** Geodynamic setting in the Alhabia Basin in late Serravallian, **b** late Tortonian and **c** present day stages. The gravity residual anomaly map is superposed in the present day sketch

Alhamilla), as well as the development of dextral strike-slip faults and NW–SE trending normal faults since late Miocene times. Faulted synform developed E–W elongated sedimentary basins whose depocentres are located in the central or southern part. This setting favoured the E–W dextral and reverse fault formation in the weak crustal zone. At this stage, Sierra Alhamilla and Sierra de Gádor antiforms were separated by a synformal faulted structure. In this framework, Sierra de Filabres would be attached to the stable Iberian Massif, whereas Sierra Nevada moves westward, Sierra de Gádor southwestward, and Sierra Alhamilla northwestward. These displacements agree with recent fault activity affecting the elongated basins that intersect in the Alhabia basin, the activity of the Gádor–Almería basin normal faults being most remarkable. The Alhabia intramontane basin illustrates the tectonic structure interaction during late orogenic processes in a collisional mountain belt.

Acknowledgements We acknowledge the comments of Dr. Fernando Bohoyo and Dr. Antonio Pedrera that highly improved this research. This study was funded by the CGL2016-80687-R and the RNM148 research group of the Junta de Andalucía.

References

Ayala C, Bohoyo F, Maestro A, Reguera MI, Torne M, Rubio F, Fernàndez M, García-Lobón JL (2016). Updated Bouguer anomalies of the Iberian Peninsula: a new perspective to interpret the regional geology. J Maps. doi:10.1080/17445647.2015.1126538

Azañón JM, Galindo-Zaldivar J, García-Dueñas V, Jabaloy A (2002) Alpine tectonics II: Betic Cordillera and Balearic Islands. In: Gibbons W, Moreno T (eds) The geology of Spain, London, pp 401–416

Braga JC, Martín JM, Quesada C (2003) Patterns and average rates of late Neogene–Recent uplift of the Betic Cordillera, SE Spain. Geomorphology 50:3–26. doi:10.1016/S0169-555X(02)00205-2

Burg JP, Podladchikov Y (1999) Lithospheric scale folding: numerical modelling and application to the Himalayan syntaxes. Int J Earth Sci 88:190–200. doi:10.1007/s005310050259

Calvert A, Sandvol E, Seber D, Barazangi M, Roecker S, Mourabit T, Vidal F, Alguacil G, Jabour N (2000) Geodynamic evolution of the lithosphere and upper mantle beneath the Alboran region of the western Mediterranean: constraints from travel time tomography. J Geophys Res Solid Earth 105:10871–10898. doi:10.1029/2000JB900024

Carmignani L, Conti P, Cornamusini G, Meccheri M (2004) The internal Northern Apennines, the northern Tyrrhenian sea and the Sardinia-Corsica block. Geol Italy Spec Vol Ital Geol Soc IGC 32:59–77

Do Couto D, Gumiaux C, Augier R, Lebret N, Folcher N, Jouannic G, Jolivet L, Suc JP, Gorini C (2014) Tectonic inversion of an asymmetric graben: insights from a combined field and gravity survey in the Sorbas basin. Tectonics 33:1360–1385. doi:10.1002/2013TC003458

Echeverria A, Khazaradze G, Asensio E, Gárate J, Dávila JM, Suriñach E (2013) Crustal deformation in eastern Betics from CuaTeNeo GPS network. Tectonophysics 608:600–612. doi:10.1016/j.tecto.2013.08.020

Galindo-Zaldivar J (1986) Etapas de fallamiento neógenas en la mitad occidental de la depresión de Ugijar (Cordilleras Béticas). Estud Geol 42:1–10. doi:10.3989/egeol.86421731

Galindo-Zaldivar J, Gil AJ, Sanz de Galdeano C, Lacy MC, García-Armenteros JA, Ruano P, Ruiz AM, Martínez-Martos M, Alfaro P (2015) Active shallow extension in central and eastern Betic Cordillera from CGPS data. Tectonophysics 663:290–301. doi:10.1016/j.tecto.2015.08.035

Galindo-Zaldívar J, Gil AJ, Borque MJ, González-Lodeiro F, Jabaloy A, Marín-Lechado C, Ruano P, Sanz de Galdeano C (2003) Active faulting in the internal zones of the central Betic Cordilleras (SE, Spain). J Geodyn 36:239–250. doi:10.1016/S0264-3707(03)00049-8

García AF, Zhu Z, Ku TL, Sanz de Galdeano C, Chadwick OA, Montero JC (2003) Tectonically driven landscape development within the eastern Alpujarran Corridor, Betic cordillera, SE Spain (Almeria). Geomorphology 50:83–110. doi:10.1016/S0169-555X(02)00209-X

García-Tortosa FJ, Sanz de Galdeano C (2007) Evidencias geomorfológicas de actividad tectónica cuaternaria en el frente montañoso del borde sur de Sierra Nevada: la falla normal de Laujar de Andarax. Cuaternario y geomorfología. Revista de la Sociedad Española de Geomorfología y Asociación Española para el Estudio del Cuaternario 21:101–112

Giaconia F, Booth-Rea G, Martínez-Martínez JM, Azañón JM, Pérez-Peña JV, Pérez-Romero J, Villegas I (2012) Geomorphic evidence of active tectonics in the Sierra Alhamilla (eastern Betics, SE Spain). Geomorphology 145:90–106. doi:10.1016/j.geomorph.2011.12.043

Gonzalez-Castillo L, Galindo-Zaldivar J, de Lacy MC, Borque MJ, Martinez-Moreno FJ, García-Armenteros JA, Gil AJ (2015) Active rollback in the Gibraltar Arc: evidences from CGPS data in the western Betic Cordillera. Tectonophysics 663:310–321. doi:10.1016/j.tecto.2015.03.010

Guest B, Horton BK, Axen GJ, Hassanzadeh J, McIntosh WC (2007) Middle to late Cenozoic basin evolution in the western Alborz Mountains: implications for the onset of collisional deformation in northern Iran. Tectonics. doi:10.1029/2006TC002091

Gurer A, Gürer ÖF, Pinçe A, Ilkisik OM (2001) Conductivity structure along the Gediz graben, west Anatolia, Turkey: tectonic implications. Int Geol Rev 43:1129–1144. doi:10.1080/00206810109465065

Instituto Geográfico Nacional, IGN (1976) Mapa de anomalías de Bouguer. Escala 1:500000. IGN, Madrid

Jabaloy A, Galindo-Zaldivar J, González-Lodeiro F (1993) The Alpujárride-Nevado-Fibábride extensional shear zone, Betic Cordillera, SE Spain. J Struct Geol 15:555–569. doi:10.1016/0191-8141(93)90148-4

Jacobs J, Thomas RJ (2004) Himalayan-type indenter-escape tectonics model for the southern part of the late Neoproterozoic–early Paleozoic East African–Antarctic orogen. Geology 32:721–724. doi:10.1130/G20516.1

Kane MF (1962) A comprehensive system of terrain corrections using a digital computer. Geophysics 27:455–462. doi:10.1190/1.1439044

Kleverlaan K (1987) Gordo megabed: a possible seismite in a Tortonian submarine fan, Tabernas basin, Province Almeria, southeast Spain. Sediment Geol 51:165–180. doi:10.1016/0037-0738(87)90047-9

Kleverlaan K (1989) Three distinctive feeder-lobe systems within one time slice of the Tortonian Tabernas fan, SE Spain. Sedimentology 36:25–45. doi:10.1111/j.1365-3091.1989.tb00818.x

Li Q, Ruano P, Pedrera-Parias A, Galindo-Zaldivar J (2012) Estructura de la cuenca sedimentaria de Tabernas-Sorbas mediante prospección gravimétrica y magnética (Zonas Internas, Cordillera Bética Oriental). Geogaceta 52:117–120

Mancilla FdL, Stich D, Berrocoso M, Martín R, Morales J, Fernandez-Ros A, Páez R, Pérez-Peña A (2013) Delamination in the Betic range: deep structure, seismicity, and GPS motion. Geology 41:307–310. doi:10.1130/G33733.1

Marín-Lechado C, Galindo-Zaldivar J, Rodríguez-Fernández LR, Serrano I, Pedrera A (2005) Active faults, seismicity and stresses in an internal boundary of a tectonic arc (Campo de Dalías and Níjar, southeastern Betic Cordilleras, Spain). Tectonophysics 396:81–96. doi:10.1016/j.tecto.2004.11.001

Marín-Lechado C, Galindo-Zaldivar J, Rodríguez-Fernández LR, Pedrera A (2007) Mountain front development by folding and crustal thickening in the Internal Zone of the Betic Cordillera-Alboran Sea boundary. Pure Appl Geophys 164:1–21. doi:10.1007/s00024-006-0157-4

Martín J, Braga JC (1994) Messinian events in the Sorbas Basin in southeastern Spain and their implications in the recent history of the Mediterranean. Sediment Geol 90:257–268. doi:10.1016/0037-0738(94)90042-6

Martín-Algarra A, Mazzoli S, Perrone V, Rodríguez-Cañero R, Navas-Parejo P (2009) Variscan tectonics in the Malaguide Complex (Betic Cordillera, southern Spain): stratigraphic and structural Alpine versus pre-Alpine constraints from the Ardales area (Province of Malaga). I. Stratigraphy. J Geol 117:241–262. doi:10.1086/597364

Martínez-Díaz JJ (2000) Actividad neotectónica en el sureste de Almería y su incidencia en la morfotectónica de la zona (Cordilleras Béticas). Rev Soc Geol España 13:417–429

Martínez-Díaz JJ, Hernández-Enrile JL (2004) Neotectonics and morphotectonics of the southern Almería region (Betic

Cordillera-Spain) kinematic implications. Int J Earth Sci 93:189–206. doi:10.1007/s00531-003-0379-y

Martínez-Martínez JM (2006) Lateral interaction between metamorphic core complexes and less-extended, tilt-block domains: the Alpujarras strike-slip transfer fault zone (Betics, SE Spain). J Struct Geol 28:602–620. doi:10.1016/j.jsg.2006.01.012

Martínez-Martínez JM, Booth-Rea G, Azañón JM, Torcal F (2006) Active transfer fault zone linking a segmented extensional system (Betics, southern Spain): Insight into heterogeneous extension driven by edge delamination. Tectonophysics 422:159–173. doi:10.1016/j.tecto.2006.06.001

Martínez-Moreno FJ, Galindo-Zaldivar J, Pedrera A, Teixidó T, Peña JA González-Castillo L (2015) Regional and residual anomaly separation in microgravity maps for cave detection: the case study of Gruta de las Maravillas (SW Spain). J Appl Geophys 114:1–11. doi:10.1016/j.jappgeo.2015.01.001

Martínez-Moreno FJ, Galindo-Zaldívar J, González-Castillo L, Azañón JM (2016) Collapse susceptibility map in abandoned mining areas by microgravity survey: a case study in Candado hill (Málaga, southern Spain). J Appl Geophys 130:101–109. doi:10.1016/j.jappgeo.2016.04.017

Nagy D (1966) The gravitational attraction of a right rectangular prism. Geophysics 31:362–371. doi:10.1190/1.1439779

Pedley RC, Busby JP, Dabek ZK (1993) GRAVMAG user manual–interactive 2.5 D gravity and magnetic modelling. British Geological Survey, Technical Report WK/93/26/R. 73

Pedrera A, Marín-Lechado C, Galindo-Zaldivar J, Rodríguez-Fernández LR, Ruiz-Constán A (2006) Fault and fold interaction during the development of the Neogene-Quaternary Almería-Níjar basin (SE Betic Cordilleras), vol 262. Geological Society, London, Special Publications, London, pp 217–230. doi:10.1144/GSL.SP.2006.262.01.13

Pedrera A, Galindo-Zaldívar J, Sanz de Galdeano C, LÃ³pez-Garrido AC (2007) Fold and fault interactions during the development of an elongated narrow basin: the Almanzora Neogene-Quaternary Corridor (SE Betic Cordillera, Spain). Tectonics. doi:10.1029/2007TC002138

Pedrera A, Galindo-Zaldívar J, Ruiz-Constán A, Duque C, Marín-Lechado C, Serrano I (2009) Recent large fold nucleation in the upper crust: insight from gravity, magnetic, magnetotelluric and seismicity data (Sierra de Los Filabres–Sierra de Las Estancias, Internal Zones, Betic Cordillera). Tectonophysics 463:145–160. doi:10.1016/j.tecto.2008.11.018

Pedrera A, Galindo-Zaldívar J, Marín-Lechado C, García-Tortosa FJ, Ruano P, Garrido AL, Azañón JM, Peláez JA, Giaconia, F (2012) Recent and active faults and folds in the central-eastern Internal Zones of the Betic Cordillera/Las fallas y pliegues recientes y activos de la parte centro-oriental de las Zonas Internas de la Cordillera Bética. J Iber Geol. doi:10.5209/rev_JIGE.2012v38.n1.39213

Rodríguez-Fernández J, Sanz de Galdeano C, Serrano F (1990) Le couloir des Alpujarras. In: Montenat C (ed) Les bassins Néogènes du Domaine Bétique Oriental (Espagne), Doc. Trav. IGAL, Paris, pp 87–100

Ruegg GJH (1964) Geologische onderzoekingen in het bekken van Sorbas, S Spanje. Amsterdam Geological Institut, University of Amsterdam

Ruiz Constán A, Galindo-Zaldivar J, Martínez MA, Martínez-Martos M, Pedrera-Parias A (2013) Estructura de la Cuenca de Ugíjar a partir de datos gravimétricos y magnéticos (Zonas Internas, Cordillera Bética Central). Geogaceta 54:95–98

Ruiz-Constán A, Galindo-Zaldívar J, Pedrera A, Celerier B, Marín-Lechado C (2011) Stress distribution at the transition from subduction to continental collision (northwestern and central Betic Cordillera). Geochem Geophys Geosyst. doi:10.1029/2011GC003824

Ruiz-Constán A, Pedrera A, Galindo-Zaldivar J, Pous J, Arzate J, Roldán-García FJ, Marín-Lechado J, Anahnah F (2012) Constraints on the frontal crustal structure of a continental collision from an integrated geophysical research: the central-western Betic Cordillera (SW Spain). Geochem Geophys Geosyst. doi:10.1029/2012GC004153

Sanz de Galdeano C (1989) Las fallas de desgarre del borde Sur de la cuenca de Sorbas-Tabernas (Norte de Sierra Alhamilla, Almería, Cordilleras Béticas). Boletín Geológico y Minero 100:73–85

Sanz de Galdeano C (1996) The EW segments of the contact between the External and Internal Zones of the Betic and Rif Cordilleras and the EW corridors of the Internal Zone (a combined explanation). Estud Geol 52:123–136

Sanz de Galdeano C, Alfaro P (2004) Tectonic significance of the present relief of the Betic Cordillera. Geomorphology 63:175–190. doi:10.1016/j.geomorph.2004.04.002

Sanz de Galdeano C, Vera JA (1991) Una propuesta de clasificación de las cuencas neógenas béticas. Acta Geológica Hispánica 26:205–227

Sanz de Galdeano C, Vera JA (1992) Stratigraphic record and palaeogeographical context of the Neogene basins in the Betic Cordillera, Spain. Basin Res 4:21–36. doi:10.1111/j.1365-2117.1992.tb00040.x

Sanz de Galdeano C, Rodriguez-Fernandez J, López-Garrido AC (1985) A strike-slip fault corridor within the Alpujarra Mountains (Betic Cordilleras, Spain). Geol Rundsch 74:641–655. doi:10.1007/BF01821218

Sanz de Galdeano C, Galindo-Zaldivar J, Morales S, López-Chicano M, Azañón JM, Martín-Rosales W (2008) Travertinos ligados a fallas: ejemplos del desierto de Tabernas (Almería, Cordillera Bética). Geogaceta 45:31–34

Sanz de Galdeano C, Shanov S, Galindo-Zaldivar J, Radulov A, Nikolov G (2010) A new tectonic discontinuity in the Betic Cordillera deduced from active tectonics and seismicity in the Tabernas Basin. J Geodyn 50:57–66. doi:10.1016/j.jog.2010.02.005

Soria JM (1998) La Cuenca de Antepaís Norbética en la Cordillera Bética Central (sector del Mencal): evolución tectosedimentaria e historia de la subsidencia. Rev Soc Geol España 11:23–31

Tarı U, Tüysüz O, Can Genç Ş, İmren C, Blackwell BA, Lom N, Tekeşin Ö, Üsküplü S, Erel L, Atiok S, Beyhan M (2013) The geology and morphology of the Antakya Graben between the Amik Triple Junction and the Cyprus Arc. Geodin Acta 26:27–55. doi:10.1080/09853111.2013.858962

Telford WM, Geldart LP, Sheriff RE (1990) Applied geophysics. Cambridge University Press, Cambridge

Torné M, Banda E (1992) Crustal thinning from the Betic Cordillera to the Alboran Sea. Geo-Mar Lett 12:76–81. doi:10.1007/BF02084915

Vera JA (2000) El Terciario de la Cordillera Bética: estado actual de conocimientos. Rev Soc Geol España 13:345–373

Weijermars R, Roep TB, Eeckhout B, Postma G, Kleverlaan K (2007) Uplift history of a Betic fold nappe inferred from Neogene-Quaternary sedimentation and tectonics (in the Sierra Alhamilla and Almeria, Sorbas and Tabernas Basins of the Betic Cordilleras, SE Spain). Geol Mijnbouw 64:345–373

Yilmaz M, Gelisli K (2003) Stratigraphic–structural interpretation and hydrocarbon potential of the Alaşehir Graben, western Turkey. Pet Geosci 9:277–282. doi:10.1144/1354-079302-539

Zagorčev IS (1992) Neotectonics of the central parts of the Balkan Peninsula: basic features and concepts. Geol Rundsch 81:635–654. doi:10.1007/BF01791382